Increased Magnetic Recording Read-back Resolution by Means of a Linear Passive Network

Abstract: It has been proven that the principle of superposition applies to a magnetic read-back wave-form. Consequently, each pulse can be treated as an isolated transient, and a linear passive network can be used to reduce its width. In many cases this effective increase in read-back resolution would permit an increase in the operating density. The isolated read-back pulse is first approximated by a Gaussian curve. A second approximation is effected in the frequency domain, and a table of transfer functions is obtained. A network is designed using one of the transfer functions, and the solution is given an algebraic form. One particular case is illustrated numerically and the laboratory results are shown.

Introduction

A method has been proposed to increase the recording density of a magnetic surface by inserting a network between the terminals of the read-back head to compress the pulses before entering the read amplifier. The method was proposed by C. E. Schlaepfer who implemented the network by means of active elements. G. C. Bacon further clarified the proposal and implemented it with a delay line and three operational amplifiers.

The present approach is a compromise between the previous proposals. High compressions are obtained without active elements; but to obtain equal amplitude between the input and output pulses, an extra linear amplification is required.

Read-back signal

In digital magnetic recording the read-back signal voltage obtained from a magnetic head is given by

$$e_0 = CV \frac{\partial}{\partial x} \int_{-\infty}^{\infty} D(x) M(x - x_0) dx , \qquad (1)$$

where D(x) represents the sensitivity function of the head and $M(x - x_0)$ is the change in surface magnetization (see Fig. 1).

In practice, $M(x - x_0)$ is much narrower than D(x). The sensitivity function D(x) can be considered as a linear filter which degrades $M(x - x_0)$ during the read-back process. It is desirable to design a compensating filter to be used in conjunction with the head

to eliminate this undesirable effect, thus obtaining a narrower read-back pulse. In order to obtain high reliability and low cost, the filter should consist of passive elements only.

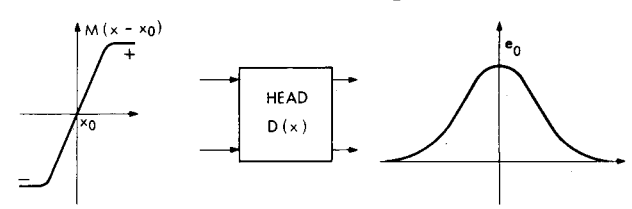
Degradation caused by the magnetic head is not harmful if the pulses are separated sufficiently. Nevertheless, as the recording density increases, the pulses appear closer together until bit crowding and bit shifting occur, see Fig. 2.

A nonreturn-to-zero type of recording will be assumed (although this is not essential). Every time a ONE occurs, the surface magnetization changes polarity and an output signal is detected by the head.

When a series of ONES is sensed, the composite readback signal (as seen on an oscilloscope) is formed by the superposition of the individual pulses.

Notice that in the composite waveform of Fig. 2 the peaks of all the pulses, except the first and the last, are separated by T, which is constant. But for the

Figure 1 Isolated read-back signal.



first and last pulses, because of the absence of a pulse which would cause symmetry, the distance between the peak of these pulses and the corresponding neighboring pulse is $T + \lambda$. In other words, these pulses appear shifted by the amount λ . The effect of this shift is an out-of-step condition with the clock signal, which in turn causes reading errors.

Also, due to the overlapping between neighboring pulses, the amplitude of each pulse is greatly diminished. This amplitude reduction imposes more rigorous requirements upon the sensing electronics, that is, in amplification and noise elimination. These undesirable effects are magnified as the density is increased.

Let us consider the following: (1) If each read-back pulse could be treated separately (in a mathematical way) regardless of whether it is really isolated or in a sequence with other pulses, and (2) if each pulse thus isolated could be compressed to the point where its effect upon neighboring pulses is negligible, then the recording density could be increased and the pulse shift λ eliminated (see Fig. 3).

Pulse isolation

Bacon and Hoagland state¹ that the principle of superposition can be applied to the overall input-output transfer process with the use of the characteristic stepfunction output response. In other words, they justify

the magnetic read-back waveform through singlepulse superposition.

In this case, each pulse can be treated separately and may be considered as a transient pulse which can be modified to fit our purposes.

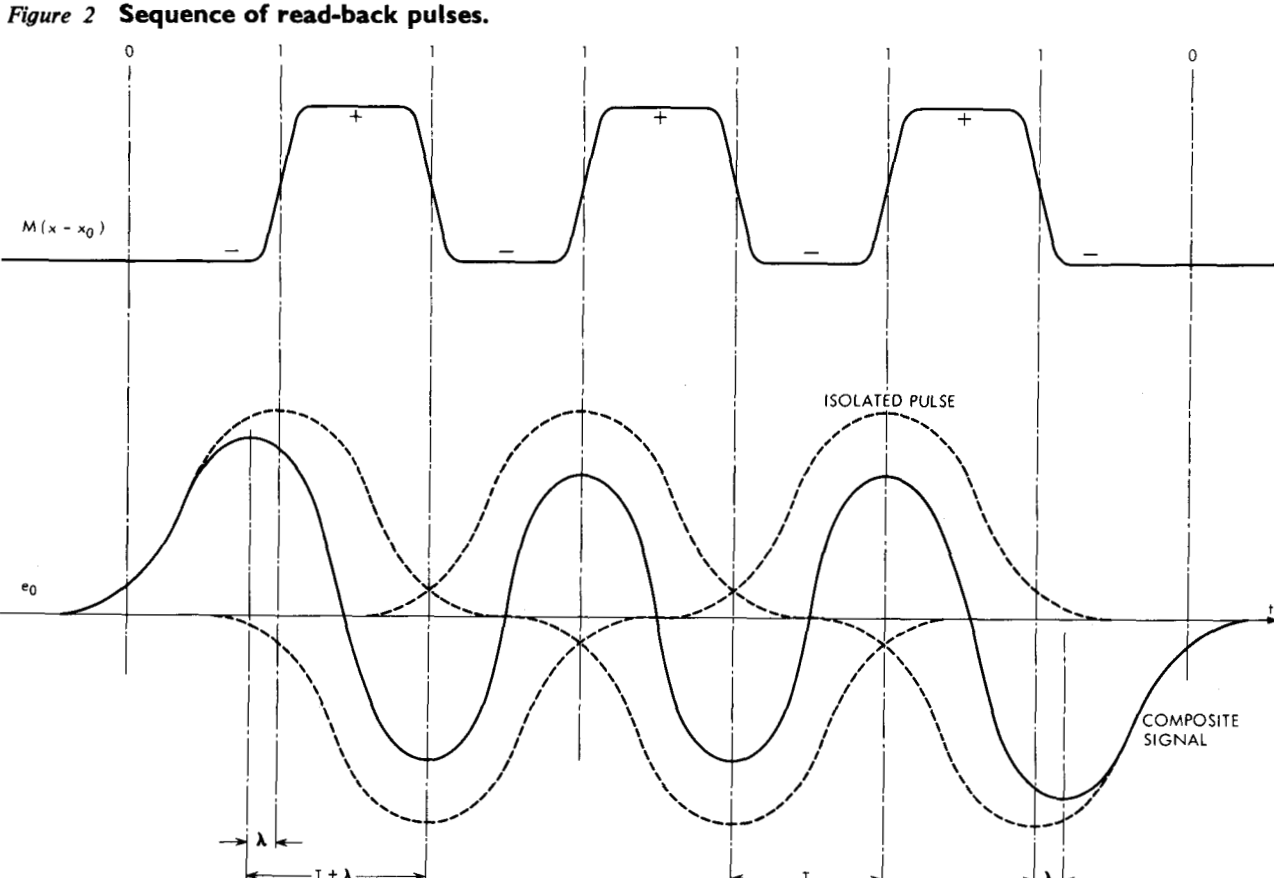
Bacon and Hoagland also state² that during readback, the existing magnetic field of the surface is extremely weak and, hence, the magnetic head will behave very nearly as a linear element.

Thus it is possible to shape the read-back pulse by means of a network composed of linear elements. It must be pointed out that this network is not a filter in the usual sense; it is not a network to discriminate certain specified frequencies (synthesis in the frequency domain), but rather a network specified by its transient behavior (synthesis in the time domain).

Let us call $f_i(t)$ the isolated signal from the read-back head, and $f_0(t)$ the desired narrower pulse. The problem can be stated: Given $f_i(t)$, find a network with a transfer function H(s) such that an output $f_0(t)$ will result (see Fig. 4).

Input signal

As stated previously, when a ONE is detected, the surface magnetization changes polarity. A typical curve $M(x - x_0)$ and output voltage from the magnetic head are shown in Figs. 1 and 2. This waveform



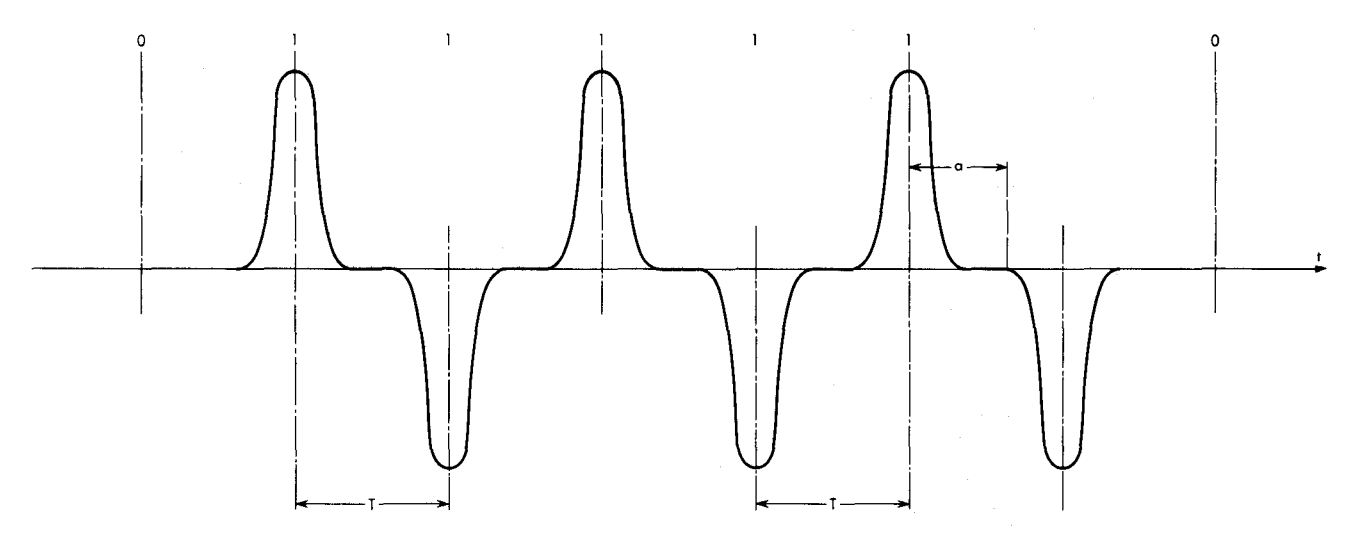


Figure 3 Sequence of read-back signals with narrowed pulses. Density can be increased by a.

resembles the normal (or Gaussian) probability density function. Indeed, this is the case, since a great number of experiments have shown that the normal curve gives the most accurate fit to the read-back signal.³

Figure 5 shows the input signal $f_i(t)$ expressed as a normal curve:

$$f_i(t) = \exp(-\xi^2 t^2). \tag{2}$$

The error at $t = \alpha$ is the value of the Gaussian function at $t = \alpha$. It is

$$\varepsilon = \exp(-\xi^2 \alpha^2) \,. \tag{3}$$

Output signal

We require only that the output signal be narrower than the input signal. A normal curve can be assumed, but with different parameters. Figure 6 shows the output signal expressed as a normal curve:

$$f_0(t) = \exp(-\eta^2 t^2)$$
 (4)

The error is

$$\varepsilon = \exp(-\eta^2 \beta^2) \ . \tag{5}$$

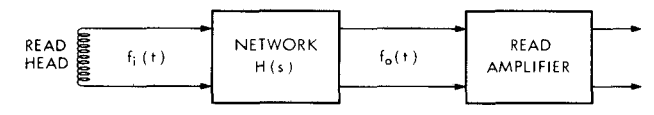
Let us define

K =desired compression ratio

$$=2\alpha/2\beta$$
, that is, $K=\alpha/\beta$. (6)

If we assume the same tolerable degree of error at

Figure 4 System diagram.



both input and output pulse edges, then Eqs. (3) and (5) give

$$\xi \alpha = \eta \beta$$

٥r

$$\xi/\eta = 1/K \ . \tag{7}$$

Transfer function

The transfer function of the network is given by

$$H(s) = F_0(s)/F_i(s) . (8)$$

Let us obtain the two-sided Laplace transform of the input pulse:

$$F_i(s) = \mathcal{L}[f_i(t)] = \int_{-\infty}^{\infty} \exp(-\xi^2 t^2) \exp(-st) dt$$
$$= (\sqrt{\pi}/\xi) \exp(s^2/4\xi^2). \tag{9}$$

Similarly

$$F_0(s) = (\sqrt{\pi/\eta}) \exp(s^2/4\eta^2)$$
 (10)

Substituting (9) and (10) in (8),

$$H(s) = (\xi/\eta) \exp[(1/\eta^2) - (1/\xi^2)] s^2/4.$$
 (11)

Substituting (7) in (11),

$$H(s) = (1/K)\exp[(1/K^2) - 1]s^2/4\xi^2.$$
 (12)

Equation (12) still contains the parameter ξ . For convenience, let us normalize the input pulse by making $\xi = 1$. Equation (12) reduces to

$$H(s) = (1/K)\exp[(1/K^2) - 1]s^2/4.$$
 (13)

In this case, for t = 2 seconds

$$f_i(2) = \varepsilon = \exp(-2^2) = 0.018$$
,

since Max $[f_i(t)] = f_i(0) = 1$, the error ε is only 1.8%

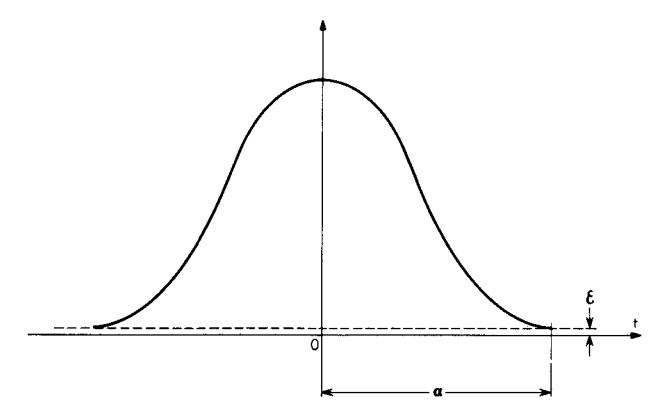


Figure 5 Input signal as a normal curve, $f_i(t) = \exp(-\xi^2 t^2)$.

of the maximum value of $f_i(t)$. Therefore, the normalized input pulse has a half-width (to be adjusted later)

 $\alpha_n = 2$ seconds.

Let us call

$$\phi^2 = (K^2 - 1)/4K^2 \,, \tag{14}$$

that is

$$\phi = \sqrt{K^2 - 1/2}K \ . \tag{15}$$

Substituting (14) in (13),

$$H(s) = (1/K)\exp(-\phi^2 s^2)$$
. (16)

Since the transfer function given by Eq. (16) is transcendental, it must be approximated by a ratio of polynomials in s. Nevertheless such approximations give non-Hurwitz polynomials in the denominator because the polynomials are even, and the roots of such polynomials have quadrantal symmetry. Instead of the transfer function, another function must be approximated. In this particular case it is possible to approximate the magnitude function and still obtain accurate results in the time domain.

For $s = i\omega$, Eq. (16) becomes

$$H(j\omega) = (1/K)\exp(\phi^2\omega^2), \qquad (17)$$

and since the imaginary component is zero, (17) is also the magnitude function

$$|H(j\omega)| = (1/K)\exp(\phi^2\omega^2), \qquad (18)$$

and by the same reason the phase is

$$Arg H(j\omega) = 0^0. (19)$$

The magnitude functions of the input and output pulses are, by (9) and (10),

$$|F_i(j\omega)| = \sqrt{\pi} \exp(-\omega^2/4) \tag{20}$$

$$|F_0(j\omega)| = (\sqrt{\pi}/K)\exp(-\omega^2/4K^2)$$
. (21)

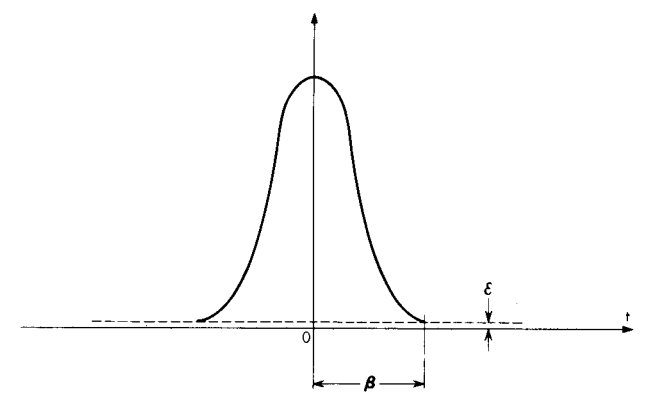


Figure 6 Output signal as a normal curve, $f_0(t) = \exp(-\eta^2 t^2)$.

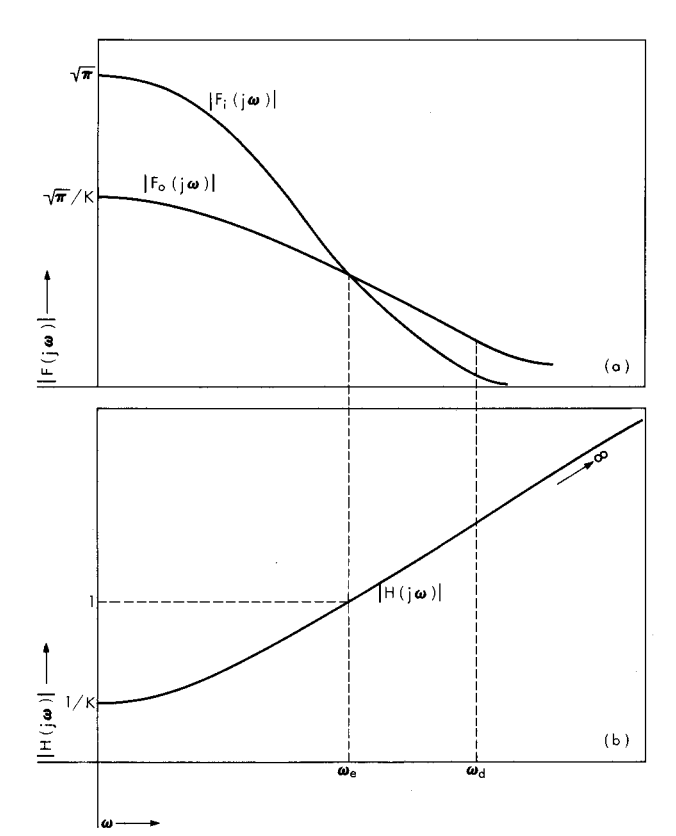


Figure 7 Curves of the magnitude functions.

Curves of Eqs. (18), (20) and (21) are given in Fig. 7. To obtain the frequency ω_e at which $|F_i(j\omega)| = |F_0(j\omega)|$, we must solve the equation

$$\sqrt{\pi} \exp(-\omega_e^2/4) = (\sqrt{\pi}/K) \exp(-\omega_e^2/4K^2)$$
, which gives

$$\omega_e = 2K[\ln K/(K^2 - 1)]^{1/2}. \tag{22}$$

To obtain realizable transfer functions, the approxi-

25

mations to $|H(j\omega)|$ must be bandwidth limited; that is, every approximation will hold only up to a frequency ω_d . If the network is going to be realized with passive elements only, and with the same impedance level, for $\omega_d > \omega_e$ it will be necessary to introduce some

attenuation factor A.

From (18) we can obtain the magnitude squared function, which is

$$|H(j\omega)|^2 = (1/K^2)\exp(2\phi^2\omega^2)$$
 (23)

Table 1 Approximations to H(s)H(-s).

N	H(s)H(-s)	Zeros	Poles
2	$\left(\frac{1}{K^2}\right)\frac{1}{1+2\phi^2s^2}$		$\frac{1}{\phi} (0 \pm j0.70710678)$
3	$\left(\frac{1}{K^2}\right)\frac{1 - \phi^2 s^2}{1 + \phi^2 s^2}$	$\frac{1}{\phi}(\pm 1 + j0)$	$\frac{1}{\phi}(0\pm j1)$
4	$\left(\frac{1}{K^2}\right)\frac{3 - 2\phi^2 s^2}{3 + 4\phi^2 s^2 + 2\phi^4 s^4}$	$\frac{1}{\phi} (\pm 1.22474487 + j0)$	$\frac{1}{\phi} (\pm 0.3352200067 \\ \pm j1.054690705)$
5	$\left(\frac{1}{K^2}\right)\frac{3 - 3\phi^2s^2 + \phi^4s^4}{3 + 3\phi^2s^2 + \phi^4s^4}$	$\frac{1}{\phi} (\pm 1.271229882 \\ \pm j0.340625032)$	$\frac{1}{\phi} (\pm 0.340625032 \\ \pm j1.271229882)$
6	$\left(\frac{1}{K^2}\right)\frac{15 - 12\phi^2 s^2 + 3\phi^4 s^4}{15 + 18\phi^2 s^2 + 9\phi^4 s^4 + 2\phi^6 s^6}$	$\frac{1}{\phi} (\pm 1.45534667 \\ \pm j0.343560805)$	$\frac{1}{\phi}(0 \pm j1.34867233)$ $\frac{1}{\phi}(\pm 0.587391538$ $\pm j1.29829514)$
7	$\left(\frac{1}{K^2}\right)\frac{15 - 15\phi^2s^2 + 6\phi^4s^4 - \phi^6s^6}{15 + 15\phi^2s^2 + 6\phi^4s^4 + \phi^6s^6}$	$\frac{1}{\phi} (\pm 1.52387182 + j0)$ $\frac{1}{\phi} (\pm 1.47994076$ $\pm j0.5927200616)$	$\frac{1}{\phi} (0 \pm j1.52387182)$ $\frac{1}{\phi} (\pm 0.5927200616$ $\pm j1.47994076)$
8	$\left(\frac{1}{K^2}\right)\frac{105 - 90\phi^2 s^2 + 30\phi^4 s^4 - 4\phi^6 s^6}{105 + 120\phi^2 s^2 + 60\phi^4 s^4 + 16\phi^6 s^6 + 2\phi^8 s^8}$	$\frac{1}{\phi} (\pm 1.680548372 + j0)$ $\frac{1}{\phi} (\pm 1.64112335$ $\pm j0.596160249)$	$\frac{1}{\phi} (\pm 0.79700116 \\ \pm j1.497202089)$ $\frac{1}{\phi} (\pm 0.250044024 \\ \pm j1.56720106)$
9	$\left(\frac{1}{K^2}\right)\frac{105 - 105\phi^2s^2 + 45\phi^4s^4 - 10\phi^6s^6 + \phi^8s^8}{105 + 105\phi^2s^2 + 45\phi^4s^4 + 10\phi^6s^6 + \phi^8s^8}$	$\frac{1}{\phi} (\pm 1.6572801 \\ \pm j0.801741003)$ $\frac{1}{\phi} (\pm 1.72038868 \\ \pm j0.252045949)$	$\frac{1}{\phi} (\pm 0.801741003 \\ \pm j1.6572801)$ $\frac{1}{\phi} (\pm 0.252045949 \\ \pm j1.72038868)$

^{*} These expressions have poles in the imaginary axis, cannot be decomposed and, therefore, cannot be implemented in realizable networks.

To approximate (23) by a ratio of polynomials in ω , we have chosen the approximation by means of a continued fraction expansion because it offers very fast convergence. Let us call

$$z = 2\phi^2 \omega^2 . (24)$$

Substituting in (23),

$$|H(z)|^2 = (1/K^2)\exp(z)$$
. (25)

The continued fraction expansion of $\exp(z)$ is given⁵

$$|H(z)|^{2} = (1/K^{2})\exp(z).$$
(25)
The continued fraction expansion of $\exp(z)$ is given⁵ by
$$\exp(z) = \frac{1}{1-z}$$

$$\frac{z}{1+z}$$

$$\frac{z}{2}$$

$$\frac{z}{1-z}$$

$$\frac{z}{6}$$

$$\frac{z}{1-z}$$

$$\frac{z}{10}$$

$$\frac{z}{1-z}$$

$$\frac{z}{1-z}$$

$$\frac{z}{10}$$

$$\frac{z}{1-z}$$

$$\frac{$$

If N = number of terms taken in the expansion, we obtain the following approximations to $\exp(z)$:

For
$$N = 1: \frac{1}{1}$$

For
$$N = 2: \frac{1}{1-z}$$

For
$$N = 3$$
: $\frac{1}{1 - \frac{z}{1 + \frac{z}{2}}} = \frac{1}{1 - \frac{2z}{2 + z}} = \frac{2 + z}{2 - z}$, etc.

Substituting $z = 2\phi^2 \omega^2$, we obtain

For
$$N = 1$$
: $|H(j\omega)|^2 \approx \left(\frac{1}{K^2}\right)\frac{1}{1}$

For
$$N = 2$$
: $|H(j\omega)|^2 \approx \left(\frac{1}{K^2}\right) \frac{1}{1 - 2\phi^2 \omega^2}$

For
$$N = 3$$
: $|H(j\omega)|^2 \approx \left(\frac{1}{K^2}\right) \frac{2 + 2\phi^2 \omega^2}{2 - 2\phi^2 \omega^2}$
= $\left(\frac{1}{K^2}\right) \frac{1 + \phi^2 \omega^2}{1 + \phi^2 \omega^2}$, etc.

Substituting $s = j\omega$ we obtain approximations to H(s)H(-s):

For
$$N = 1$$
: $H(s)H(-s) \approx \left(\frac{1}{K^2}\right)\frac{1}{1}$

For
$$N = 2$$
: $H(s)H(-s) \approx \left(\frac{1}{K^2}\right)\frac{1}{1 + 2\phi^2 s^2}$

For
$$N = 3$$
: $H(s)H(-s) \approx \left(\frac{1}{K^2}\right)\frac{1 - \phi^2 s^2}{1 + \phi^2 s^2}$, etc.

A more complete list is given in Table 1. The corresponding poles and zeros are also included. The approximations given in Table 1 are the diagonal entries (or stair-case entries) of the Padé table for H(s)H(-s).

From the entries of Table 1 we can take the left-half plane poles, and they will constitute the poles of H(s). In this fashion we can construct the approximate transfer functions.

$$H(s) \approx \left(\frac{1}{K}\right) \frac{(s-z_1)(s-z_2)\cdots(s-z_n)}{(s-P_1)(s-P_2)\cdots(s-P_m)}.$$

Computer simulation

To determine the degree of approximation to the output pulse which was achieved by the entries in the table, a FORTRAN program was written to carry out the convolution of $f_i(t)$ and the inverse transform of H(s).

Numerical example

Let us choose K = 2. Since the normalized input pulse is $2\alpha = 4$ seconds, the desired normalized output pulse will be

 $2\alpha/K = 4/2 = 2$ seconds wide.

Substituting K = 2 in Eq. (16),

$$\phi = \sqrt{K^2 - 1/2}K = \sqrt{3/4} = 0.433012701$$
. (27)

In Table 1 let us choose the entry N = 9. Substituting the value of ϕ calculated above, we obtain the following poles and zeros for H(s)H(-s).

Poles:

$$\pm 1.85154154 \pm j3.82732446 + 0.582075188 + j3.97306747$$

Zeros:

$$\pm 3.82732446 \pm j1.85154154 + 3.97306747 + j0.582075188$$

Disregarding the right-half plane poles and the lefthalf plane zeros,* we obtain for H(s)

[•] The choice of right-half plane zeros assures a more linear phase response than would be possible with the other alternative.

Poles:

 $-1.85154154 \pm j3.82732446$ $-0.582075188 \pm j3.97306747$

Zeros:

 $+3.82732446 \pm j1.185154154 +3.97306747 \pm j0.582075188$

Since we have right-half plane zeros, our transfer function is nonminimum-phase. The output pulse $f_0(t)$ will be delayed with respect to $f_i(t)$. This delay is quite tolerable since all the read-back pulses will be delayed by the same amount, but the relative distance between adjacent pulses will remain unchanged.

With the poles and zeros calculated above, we obtain the transfer function

$$H(s) = \left(\frac{1}{2}\right) \frac{\left[(s - 3.82732446)^2 + (1.85154154)^2\right] \left[(s - 3.97306747)^2 + (0.582075188)^2\right]}{\left[(s + 1.85154154)^2 + (3.82732446)^2\right] \left[(s + 0.582075188)^2 + (3.97306747)^2\right]}$$

that is

$$H(s) = \left(\frac{1}{2}\right) \frac{s^4 - 15.60078386s^3 + 95.02556847s^2 - 267.0633964s + 291.4687835}{s^4 + 4.867233456s^3 + 38.51164079s^2 + 80.7526977s + 291.4687835}.$$
 (28)

The empirical input signal $f_i(t)$ convolved with the inverse Laplace transform of (28) gives an output pulse of $f_0(t)$. The result obtained from the computer is shown in Fig. 8. The maximum value of $f_0(t)$ has been normalized to 1. It is seen that the delay is 1.26 seconds. The width of the output pulse is 2 seconds, as expected.

In a similar fashion it is possible to calculate from Table 1 approximate transfer functions with either left-plane or right-half plane locations for the zeros. This was done, and every possible transfer function was convolved with $f_i(t)$. For K=2 the entry N=9, illustrated above, offered the best accuracy with a reasonable number of terms.

The pole and zero configuration is:

Poles

 $-1.85154154 \pm j3.82732446$ $-0.582075188 \pm j3.97306747$

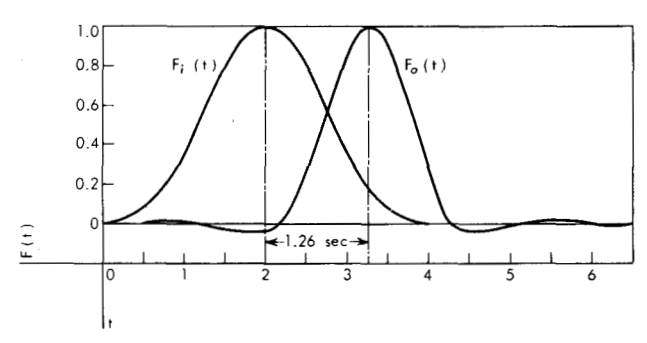
Zeros:

 $+3.82732446 \pm j1.85154154 +3.97306747 \pm j0.582075188$

Frequency response

Although we are primarily interested in the timedomain behavior of the transfer function, it is

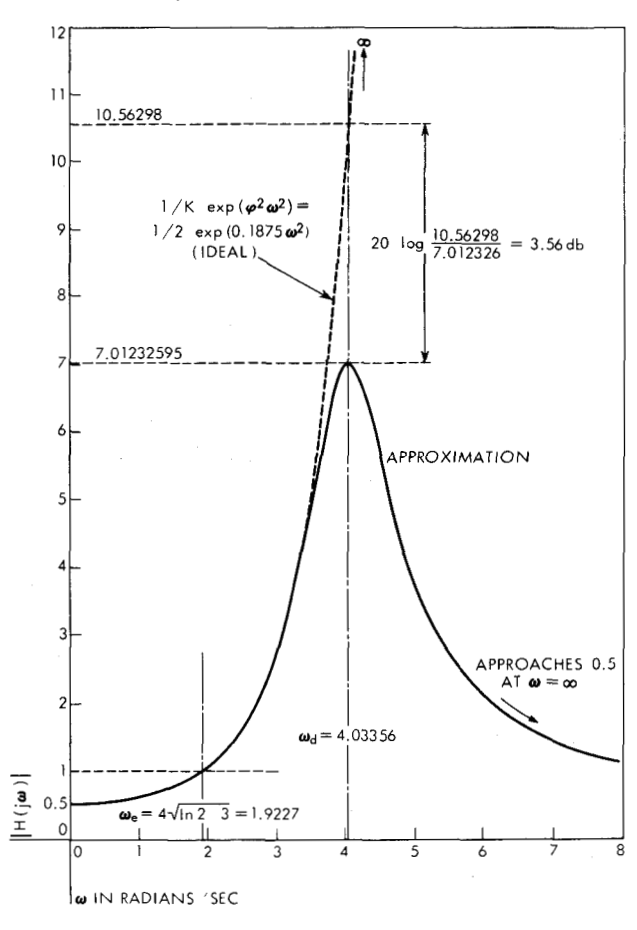
Figure 8 Computer simulation.



necessary to calculate the magnitude and phase of the transfer function to verify our approximation to the magnitude function. Also, we must observe the phase very carefully since it has been ignored up to this point.

In Eq. (28) let us make $s = j\omega$. We obtain

Figure 9 Magnitude vs frequency.



$$H(j\omega) = \left(\frac{1}{2}\right) \frac{(\omega^4 - 95.02556847\omega^2 + 291.4687835) + j(15.60078386\omega^3 - 267.0633964\omega)}{(\omega^4 - 38.51164079\omega^2 + 291.4687835) + j(-4.867233456\omega^3 + 80.75269772\omega)}$$

The magnitude function is

$$\left|H(j\omega)\right| = \left(\frac{1}{2}\right) \left[\frac{(\omega^4 - 95.02556847\omega^2 + 291.4687835)^2 + (15.60078386\omega^3 - 267.0633964\omega)^2}{(\omega^4 - 38.51164079\omega^2 + 291.4687835)^2 + (4.86723345\omega^3 - 80.75269772\omega)^2}\right]^{\frac{1}{2}}.$$

Evaluating $|H(j\omega)|$ for values of ω from zero to 8 radians/sec, we obtain Fig. 9. Our approximation is good only up to $\omega_d = 4.03356$ radians/sec. At this frequency we have

$$Max|H(j\omega)| = 7.01232595$$
. (29)

The phase is given by

 $Arg H(j\omega)$

$$= \arctan \frac{15.60078386\omega^3 - 267.0633964\omega}{\omega^4 - 95.02556847\omega^2 + 291.4687835}$$
$$-\arctan \frac{-4.867233456\omega^3 + 80.75269772\omega}{\omega^4 - 38.51164079\omega^2 + 291.4687835}.$$

Evaluating Arg $H(j\omega)$ for values of ω from zero to 8 radians/sec, we obtain Fig. 10. It is observed that up to the frequency of approximation, ω_d , the phase can be considered linear to an acceptable degree of accuracy.

Network synthesis

Given a particular transfer function which fulfills well-known realizability requirements, there are in general many possible networks; only one will be illustrated.

The magnetic head is connected directly to an amplifier. The network must be inserted in a desirable location. Suppose that as far as input and output terminals are concerned, the network appears as in Fig. 11. That is, the network is connected between a voltage generator and a purely resistive load. Since the insertion of the network must disturb the previous configuration as little as possible, we have chosen a constant-R configuration.

In the practical case under consideration the network is connected to a critically balanced push-pull amplifier. Consequently, it is desirable to load both lines by the same amount. Instead of a common-node network, a symmetrical lattice network will be realized (see Fig. 12).

In terms of the transfer function the branch impedances of the symmetrical lattice network are⁶

$$Z_a = \frac{1 - H(s)}{1 + H(s)} \tag{30}$$

$$Z_b = \frac{1}{Z}. (31)$$

For Z_a and Z_d to be positive real, the requirements⁷

Figure 10 Phase vs frequency.

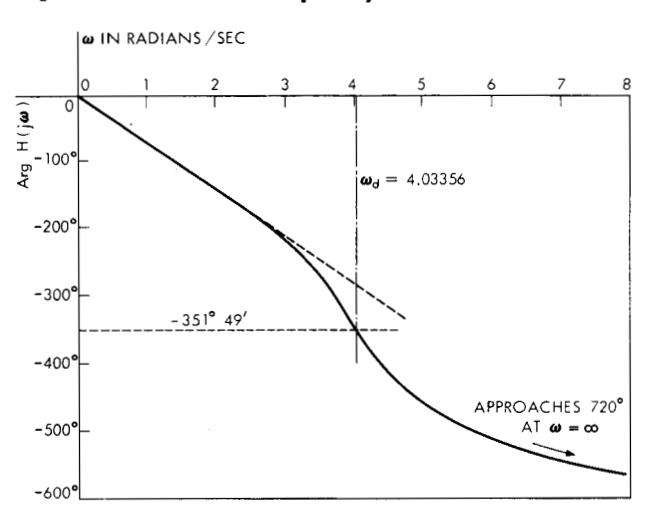


Figure 11 Input-output to the network.

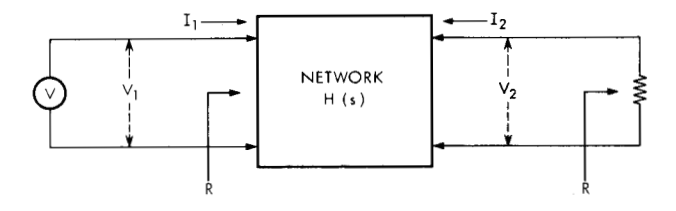
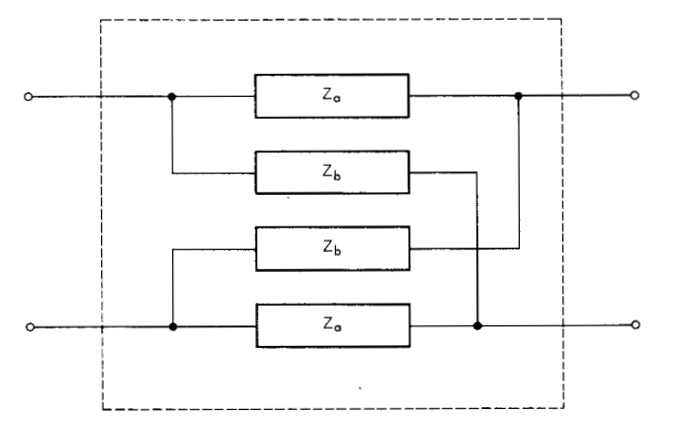


Figure 12 Symmetrical lattice network.



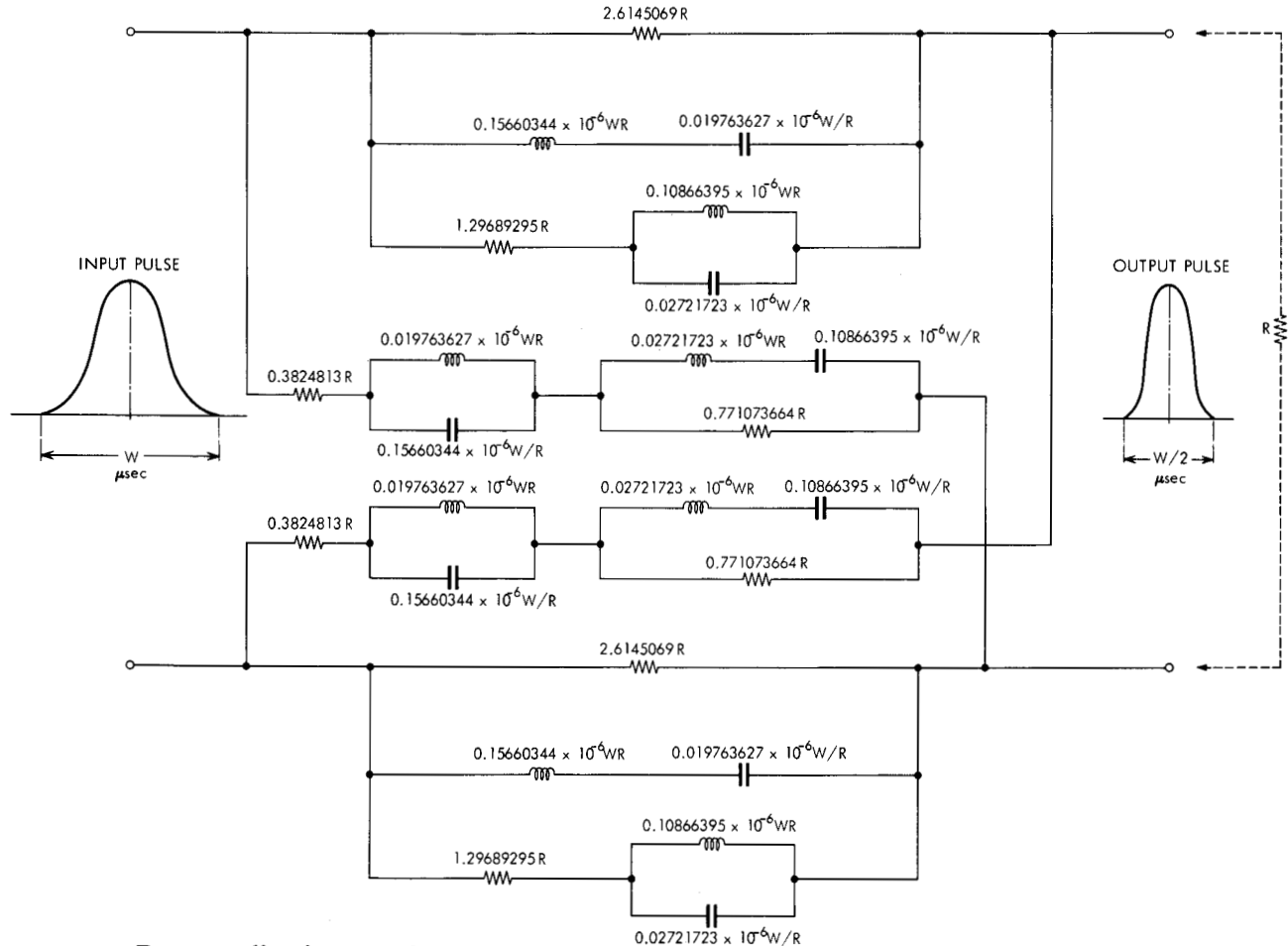


Figure 13 Denormalized network.

are that (1) H(s) has no poles in the right-half plane or on the imaginary axis and (2) $|H(j\omega)| \le 1$ for $0 \le \omega \le \infty$.

The transfer function H(s) given by Eq. (28) fulfills the first requirement since all the poles are in the left-half plane.

To fulfill the second requirement, it is necessary to multiply H(s) by

$$A \le \frac{1}{\operatorname{Max}|H(j\omega)|} \,. \tag{32}$$

Substituting (29) in (32), let us choose

$$A = 1/7.01232595, (33)$$

which gives an attenuation of $20 \log(1/A) = 16.917$ db. Multiplying (28) by (33),

$$H(s) = \frac{0.0713030175s^4 - 1.112382964s^3 + 6.775609772s^2 - 19.04242602s + 20.78260377}{s^4 + 4.867233456s^3 + 38.51164079s^2 + 80.75269772s + 291.4687835}.$$
 (34)

Substituting (34) in (30) and (31), we obtain the normalized network.

The normalized input pulse was considered 4 seconds wide. Nevertheless, this normalized width was chosen quite arbitrarily. By truncating a Gaussian approximation, we have used a pulse which starts with a step function whose height is 1.8 per cent. In practice, the pulses coming from the magnetic head do not have these step functions, that is, they approach the base line more rapidly than a Gaussian curve. This

discrepancy causes the output pulse to have overshoots as shown in Fig. 8, when an empirical input pulse is convolved with the impulse response. An adjustment of the width of the normalized input pulse is necessary.

By varying the width of the input pulse in computer simulation and in laboratory testing, it was found that these overshoots are greatly minimized, without detriment to the compression factor, by using a pulse 10 per cent wider than originally assumed.

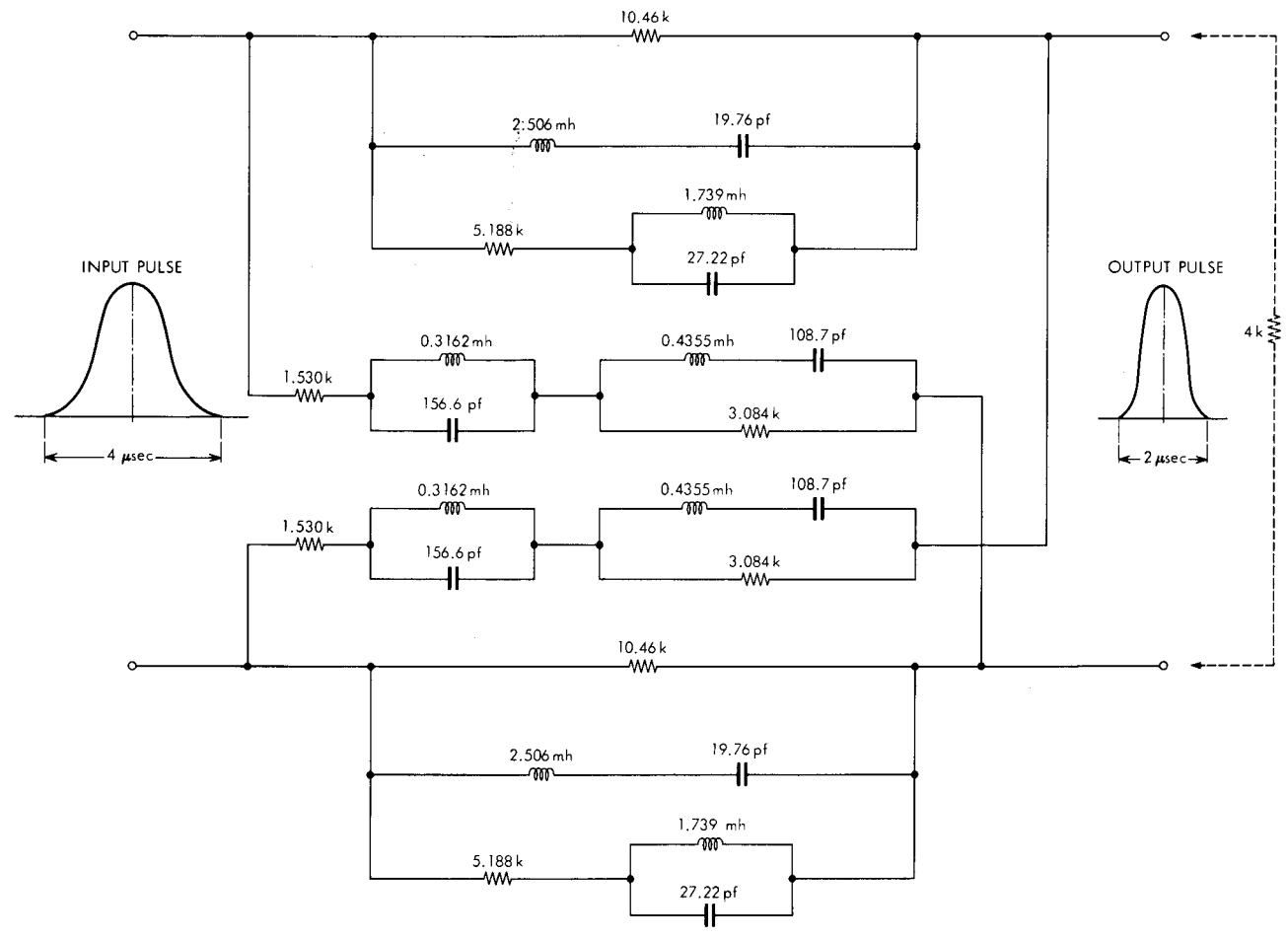


Figure 14 Network for W = 4, $R = 4 \times 10^3$.

For a pulse W microseconds wide, the frequency scaling factor is then

$$\theta = \frac{4.4 \times 10^6}{W} \,. \tag{35}$$

If R_n , L_n and C_n are normalized resistors, inductors and capacitors, the actual values will be

$$R_{\rm act} = RR_n \tag{36}$$

$$L_{\text{act}} = \frac{WRL_n}{4.4 \times 10^6} \tag{37}$$

$$C_{\text{act}} = \frac{WC_n}{4.4 \times 10^6 \times R} \,. \tag{38}$$

Applying (36), (37) and (38), we obtain the denormalized network shown in Fig. 13.

Laboratory results

Let us consider a pulse 4 microseconds wide. This pulse is fed to a linear amplifier whose input impedance is a resistance of 4 kohms. Substituting W = 4 and $R = 4 \times 10^3$ in Fig. 13, we obtain the network shown in Fig. 14.

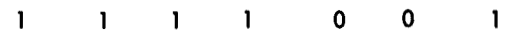
Figure 15 shows the laboratory results obtained with this network using a dual-beam oscilloscope. The magnetic head used in these experiments was originally designed for a density of 450 bits per inch.

Figure 15(a) shows the 4 microsecond input pulse, and superimposed upon it the narrowed pulse obtained from the network. The peaks of the pulses have been made to coincide on the oscilloscope.

Figure 15(b) shows a series of pulses written at 450 bpi on a disk. The narrower pulses obtained from the network are superimposed.

Figure 15(c) shows a series of pulses written at 900 bpi. The upper trace is the output from the head, and it is seen that due to pulse crowding the amplitude of adjacent pulses varies considerably. The lower trace is the output from the network, and the amplitude variation of the pulses is considerably reduced.

Figure 15(d) shows two adjacent pulses at 900 bpi. The outputs from the head and from the network are superimposed. The peaks of the pulses obtained at the head are seen to be more widely separated than the ones obtained from the network; consequently at this density the network reduces the bit-shift of the head signal.



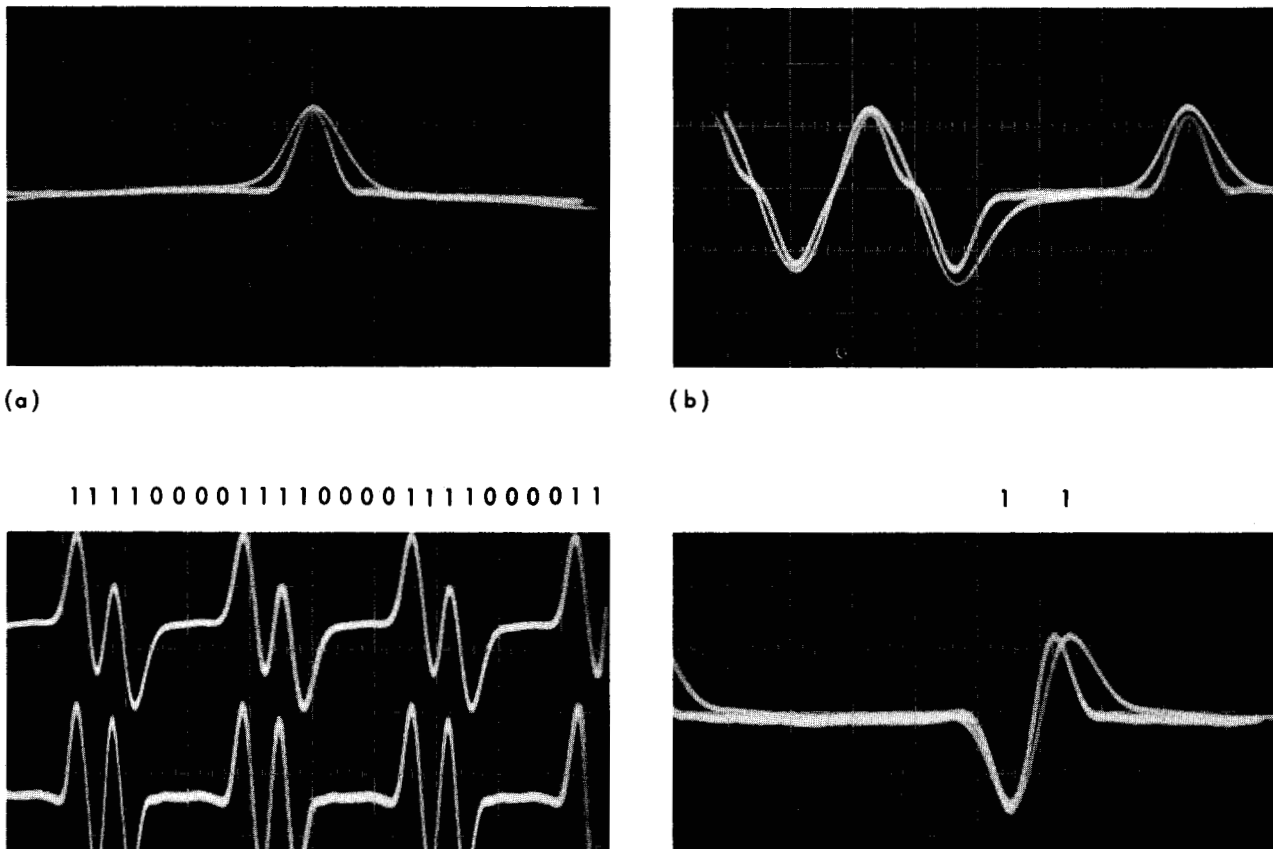


Figure 15 Oscillograms of a pulse-compression ratio of 2 to 1.

(a) Horizontal scale: 2 µsec/large division. Vertical scale: Input (wide) pulse—20 mv/large division. Output (narrow) pulse—5 mv/large division. Delay from input to output: 1.25 µsec. (b) Horizontal scale: 2 µsec/large division. Recording density: 450 bpi. (c) Horizontal scale: 5 µsec/large division. Recording density: 900 bpi. Upper trace: Network input. Lower trace: Network output. (d) Horizontal scale: 2 µsec/large division. Recording density: 900 bpi. Wide pulse: Network input. Narrow pulse: Network output.

(d)

Figure 15 offers only a qualitative, pictorial account of the network behavior. A quantitative evaluation is shown in Fig. 16. The relative amplitude of the pulses and their bit-shift are offered at several recording densities. It is seen that the amplitude obtained from the head decays after 450 bits per inch, as originally designed. Also at this density the bit-shift starts to increase. Nevertheless, with the same head, the output from the network shows that the relative amplitude of the pulses starts to decay at 900 bpi, and also at this density the bit-shift starts to increase.

Conclusions

(c)

Again it has been confirmed that the principle of superposition applies to the read-back waveform in a magnetic recording system. For our purposes the read-

back process can be considered linear.

Proper linear filtering of the signal read from a magnetic surface reduces the interference of adjacent read-back pulses, and in some cases permits an increase in recording density. A practical case has been illustrated, and the laboratory results have indicated a twofold increase in the recording density.

For this purpose a network has been designed in general form such that a network can be easily obtained for every particular application.

Acknowledgments

Many thanks are due Carl E. Schlaepfer, who not only proposed the original idea but also aroused the author's interest in this subject and provided comments and encouragement. The author is deeply

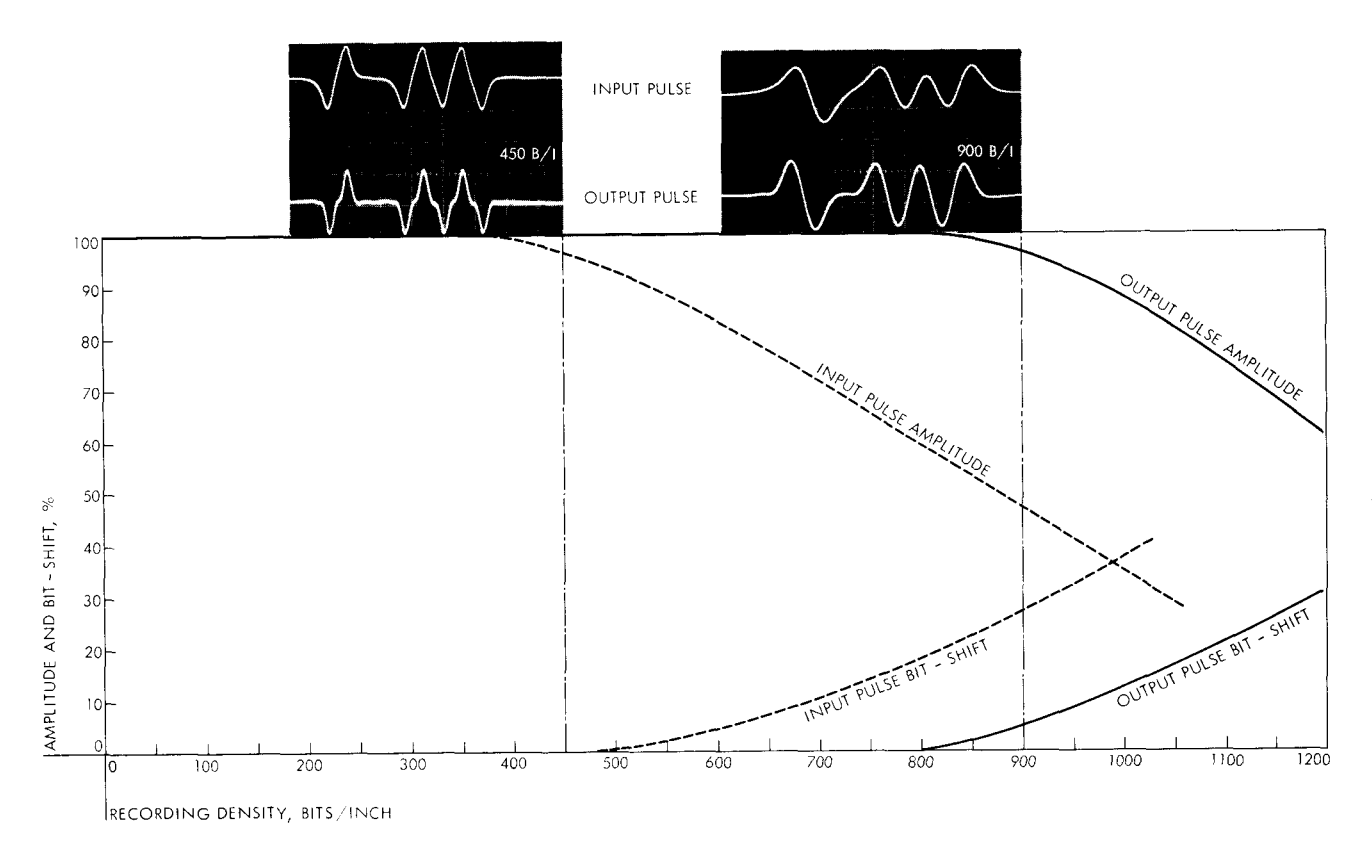


Figure 16 Amplitude and bit-shift vs recording density.

indebted to Terrence C. Kelly of the Computation Laboratory for writing all the FORTRAN programs and also for much valuable discussion and constructive criticism. Lester F. Shew provided all the magnetic recording equipment for the tests and also contributed his experience for the proper evaluation of the network performance. George G. Keller assembled, adjusted and tested all the prototype networks. His assistance has been invaluable for the practical implementation of the project.

Bibliography

- 1. A. S. Hoagland, "A Logical Reading System for Non-Return-to-Zero Magnetic Recording," IRE Transactions on Electronic Computers, EC-4, 93-95 (1955).
- 2. R. V. Churchill, Introduction to Complex Variables and Applications, McGraw Hill Book Co., 1948.
- 3. D. Jackson, Fourier Series and Orthogonal Polynomials. The Mathematical Association of America, 1941.
- 4. W. Magnus and F. Oberhettinger, Formulas and Theorems for the Functions of Mathematical Physics, Chelsea Publishing Company, 1954.
- 5. H. Bateman, Higher Transcendental Functions, McGraw-Hill Book Co., 1953, Vols. 1 and 2.
- 6. O. Perron, Die Lehre von den Kettenbruchen, Chelsea Publishing Co., 1950.
- 7. T. J. Stieltjes, "Recherches sur les Fractions Continués." Ann. Fac. Sci. Toulouse, 8, 1-122 (1894).
- P. Wynn, "The Rational Approximation of Functions Which Are Formally Defined by a Power Series Expansion,' Mathematics of Computation, April 1960, pp. 147-186.

- 9. F. Ba Hli, "A General Method for Time Domain Network Synthesis," IRE Transactions on Circuit Theory, CT-1, No. 3, 21-28 (1954).
- 10. J. G. Truxal, "Numerical Analysis for Network Design," IRE Transactions on Circuit Theory, CT-1, 49-60 (1954).
- 11. E. A. Guillemin, Synthesis of Passive Networks, John Wiley and Sons, Inc., 1957.
- D. F. Tuttle, Network Synthesis, John Wiley and Sons, Inc., 1958, Vol. 1.
- 13. N. Balabanian, Network Synthesis, Prentice-Hall, 1958.
- 14. E. S. Kuh and D. O. Pederson, Principles of Circuit Synthesis. McGraw-Hill Book Co., 1959.

References

- 1. G. C. Bacon and A. S. Hoagland, "High Density Digital Magnetic Recording Techniques," Proceedings of the IRE, 49, 1, 265 (1961).
- Ibid., p. 258-67.
 J. W. Hung, "Transfer Function and Error Probability of a Digital Magnetic Tape Recording System," J. Appl. Phys., 31, 5, 396S-397S (1960).
- M. F. Gardner and J. L. Barnes, Transients in Linear Systems, John Wiley and Sons, Inc., 1956, p. 226.
- 5. H. S. Wall, Analytic Theory of Continued Fractions, D. van Nostrand Company, 1948, p. 347.
- 6. M. E. Van Valkenburg, Introduction to Modern Network Synthesis, John Wiley and Sons, Inc., 1960, p. 348.
- A. Talbot, "A New Method of Synthesis of Reactance Networks," Proceedings of the I.E.E. (London), Part IV, Monograph No. 77, 73-90, Theorem 4, (1954).

Received May 22, 1962